

CHANNEL CONDUCTANCE OF ABA STACKING TRILAYER GRAPHENE NANORIBBON FIELD-EFFECT TRANSISTOR

HATEF SADEGHI*, M. T. AHMADI, S. M. MOUSAVI and RAZALI ISMAIL

*Electrical Engineering Faculty, Universiti Teknologi Malaysia (UTM),
81310 Skudai, Johor Darul Takzim, Malaysia
hatef.sadeghi@gmail.com

MAHDIAR H. GHADIRY

*Department of Computer Engineering, Arak Branch,
Islamic Azad University, Arak, Iran*

Received 7 November 2011

Accepted 3 January 2012

In this paper, our focus is on ABA trilayer graphene nanoribbon (TGN), in which the middle layer is horizontally shifted from the top and bottom layers. The conductance model of TGN as a FET channel is presented based on Landauer formula. Besides the good reported agreement with experimental study lending support to our model, the presented model demonstrates that minimum conductivity increases dramatically by temperature. It also draws parallels between TGN and bilayer graphene nanoribbon, in which similar thermal behavior is observed. Maxwell-Boltzmann approximation is employed to form the conductance of TGN near the neutrality point. Analytical model in degenerate regime in comparison with reported data proves that TGN-based transistor will operate in degenerate regime like what we expect in conventional semiconductors. Moreover, our model confirms that in similar condition, the conductivity of TGN is less than bilayer graphene nanoribbon as reported in some experiments.

Keywords: Conductance; trilayer graphene; model; bilayer graphene; FET.

1. Introduction

Single-layer carbon atoms with hexagonal symmetry (known as Graphene mono-layer) was reported in early 2004.^{1,2} Layers of graphene can be stacked differently depending on the horizontal shift of graphene planes. Every individual graphene multilayer sequence behaves like a new material in which different stacking of graphene sheet leads to different electronic properties.³⁻⁵ Recently, unique properties of mono- and few-layer graphene have attracted great attention, and have been proposed as promising candidates for the future nanoelectronics. Ballistic transport phenomenon at room temperature, anomalous quantum Hall effect and tunable band gap by applied perpendicular electric field and magnetic field have

been observed experimentally.^{6–11} General electronic properties of graphene-based materials are varied by increasing the number of the layers, but low energy electronic properties in graphene layers depend on a large number of parameters. Since theorists have been unable to agree about the details of the electronic structure, it needs more research to make sure about electrical properties of these materials.⁴ In addition, number and configuration of graphene layers play significant roles in realizing either metallic or semiconducting electronic behavior.^{7–9} One of the important aspects of electronic properties of graphene is its conductivity as a channel in the field-effect transistors (FETs).^{12,13} Recently, experimental attention has turned toward the properties of trilayer graphene (TG),^{9,14} and a tunable three-layer graphene single-electron transistor has been experimentally realized.^{3,15} In this paper, the conductance of ABA trilayer graphene nanoribbon (TGN) is modeled based on Landauer formula. Conductance of TGNs in the degenerate and the non-degenerate perturbations are studied as well as its temperature dependence. The analytical model in degenerate regime out of neutrality point is approximated. Moreover, near the neutrality point, Maxwell–Boltzmann approximation is discussed. Finally, a good agreement with experimental data is reported. Comparison between bilayer graphene nanoribbon (BGN) conductance model in Ref. 13 with TGN conductance model presented in this paper confirms that the conductivity of BGN is higher than TGN, which had already been reported in some experiments.⁴

Graphene layers can be arranged in different sequences. The simplest crystallographic structure is Hexagonal or AA stacking, where each layer is placed directly on top of another, however it is unstable. AB (Bernal) stacking is only one distinct stacking structure for bilayers. For trilayers, it can be formed in either ABA as shown in Fig. 1 or ABC (rhombohedral) stacking.^{16,17} Bernal stacking (ABA) is a common Hexagonal structure which has been found in graphite. However, some parts of graphite can also have rhombohedral structure (the ABC stacking).^{3,18} In this paper, we address our study to ABA stacking trilayer graphene (TG) with width less than 10 nm which can be called TGN. Note that each honeycomb contains three cells where each cell consists of two carbon atoms named A and B.

ABA TGN consists of three coupled graphene layers on the bottom, middle and top.¹⁹ For Bernal stacking TGN, B_2 atom from middle layer is directly above A_1 atom from bottom layer and below A_3 atom from top layer. The parameters γ_0 , γ_1 , γ_3 (γ_4) and γ_2 respectively describe the interaction between nearest neighbor, A_i and B_i atoms, the strong coupling between nearest layers, the weaker nearest layer coupling and the interaction between the next nearest layers.³ Very high carrier mobility can be achieved in Graphene-based materials¹⁶ which makes them promising candidates for nanoelectronics devices.²⁰ Recently electron and hole mobility as high as $2 \times 10^5 \text{ cm}^2 \text{ V}^{-1} \text{ s}^{-1}$ have been reached for suspended graphene.⁴ Also, ballistic transport has been observed up to room temperature in these materials.^{7,21} The perpendicular external applied electric or magnetic fields are

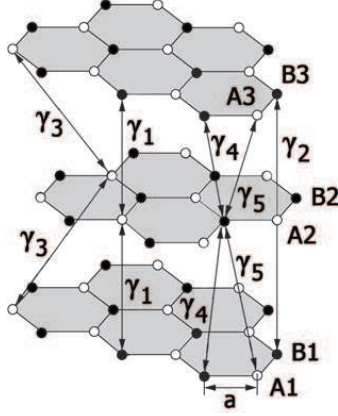


Fig. 1. Three coupled graphene layers with ABA (Bernal) stacking. $a = 0.142$ nm, the monolayer lattice constant. $\gamma_0 = 3.16$ eV (see Ref. 16) is interaction between nearest neighbor A_i and B_i atoms, $\gamma_1 = 0.44$ eV (see Ref. 4) is the strong coupling between nearest layers, γ_3 (γ_4) are the weaker nearest layer coupling and γ_2 is the interaction between the next nearest layers.

expected to induce band crossing variation in Bernal stacked TGNs.^{16,22–24} Therefore, TGN is found to be a semimetal with its behavior different from that of single-layer and BGN in some aspects. The response of ABA-stacked TGN to external electric field is different from that of mono or BGN. In fact, rather than opening a gap in BGN, the magnitude of overlap in TGN is tuned.¹⁴ On the other hand, overlap between the conduction and valence bands takes place in band structure of TGNs, which can be controlled by a perpendicular external electric field.³ The band overlap increases with increasing the external electric field, which is independent of the electric field polarity. Moreover, it is shown that effective mass remains constant when external electric field is increased.^{4,25} Spectrum of full tight-binding Hamiltonian of HOPG stacking (ABA) TGN was obtained in Refs. 19 and 25–28. The presence of electrostatic fields breaks the symmetry between the three layers. Using perturbation theory²⁹ in the limit of $v_F|k| \ll \Delta \ll t_\perp$ indicates electronic band structure of TGN as:²⁶

$$E(k) = \alpha|k| - \beta|k|^3, \quad (1)$$

where $\alpha = \sqrt{2}\Delta v_F/t_\perp$ and $\beta = \sqrt{2}v_F^3/\Delta t_\perp$, in which the upper layer is at potential Δ , the lower layer is at potential $-\Delta$, and the middle layer is at zero potential. Figure 2 shows band structure of ABA staking TGNs based on Eq. (1).

In this description, the Fermi velocity is $v_F = \sqrt{3}\gamma_0 a/2\hbar \cong 10^6$ m/s (see Ref. 3), where γ_0 (≈ 3.12 eV) (see Ref. 16) is the hopping between π orbitals located at nearest neighbor atoms. We denote the hopping integral as t_\perp ($\approx 0.1\gamma_0$) where the difference in the electrostatic potentials in the two layer graphene is 2Δ ($\Delta = vg/2$).

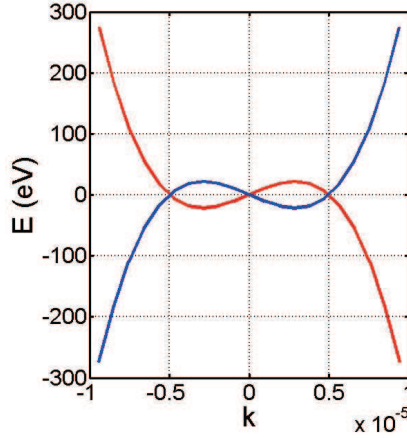


Fig. 2. Band structure of ABA staking TGNs.

The external electric field (Δ), which can change the amount of overlap in band structure of TGN, plays a significant role. Varying the band overlap by electric field is a unique property of TGN that had not been previously found in other semi-metallic systems.⁴

2. Conductance Model

For one-dimensional TGN field-effect transistor (1D TGNFET), a graphene nanoribbon channel is assumed to be ballistic, and as shown in Fig. 3, the current from source to drain can be given by the Boltzmann transport equation and therefore based on Ohm's Law, this equation can be written as Landauer formula:^{30,31}

$$G = \frac{2q^2}{h} \int_{-\infty}^{+\infty} M(E)T(E) \left(-\frac{df}{dE} \right) dE, \quad (2)$$

where q is the electron charge, h is Planck's constant, $T(E)$ is the transmission probability and f is the Fermi-Dirac distribution function. High carrier mobility

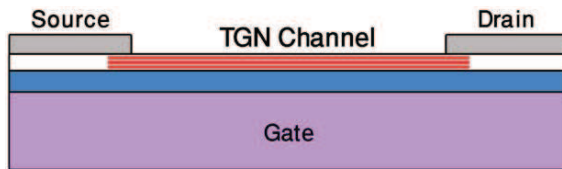


Fig. 3. Simple 1D TGNFET where TGN is used as a channel between Drain and Source. The width of TGN is assumed to be less than 10 nm in 1D form (more than 10 nm in 2D form).

reported from experiments in the graphene leads to assume a completely ballistic carrier transportation in the graphene, meaning that carriers travel over the channel without scattering which implies that average probability of injected electron at one end transmitting to the other end is approximately equal to one ($T(E) = 1$).³¹

The number of propagating modes at the Fermi energy is defined as the conductance of the clean (disorder-free) ideal nanoribbons.³¹ Each spin-degenerate propagating mode contributes to the total conductance by the conductance unit $G_0 = 2q^2/h$ (see Ref. 32). The number of modes that are above the cutoff at energy E in the transmission channel by including the spin effect is

$$M(E) = \frac{dE}{Ldk} = \frac{\alpha - 3\beta k^2}{L}, \quad (3)$$

where $L = 1$ and $L = 1/W$ for one- and two-dimensional (1D and 2D) systems, respectively, in Ballistic regime^{30,33} and W is the width of the ribbon. Number of modes incorporated with Landauer formula indicates the conductance of TGN as

$$G = \frac{2\alpha q^2}{Lh} \int_{-\infty}^{+\infty} \left(-\frac{d}{dE} \left(\frac{1}{1 + e^{\frac{E-E_F}{k_B T}}} \right) \right) dE \\ + \frac{-6\beta q^2}{Lh} \int_{-\infty}^{+\infty} k^2 \left(-\frac{d}{dE} \left(\frac{1}{1 + e^{\frac{E-E_F}{k_B T}}} \right) \right) dE, \quad (4)$$

where momentum (k) can be derived by using Cardano's solution for cubic equations.³⁴ Equation (4) can be assumed in the form of $G = N_1 G_1 + N_2 G_2$ where $N_1 = 2\alpha q^2/Lh$, $N_2 = -6\beta q^2/Lh$. Since G_1 is an odd function, its value is equivalent to zero and $G = N_2 G_2$.

$$G_2 = \int_{-\infty}^{+\infty} \left(\left(-\frac{E}{2\beta} + \sqrt{\left(\frac{-\alpha}{3\beta} \right)^3 + \left(\frac{E}{2\beta} \right)^2} \right)^{1/3} \right. \\ \left. + \left(-\frac{E}{2\beta} - \sqrt{\left(\frac{-\alpha}{3\beta} \right)^3 + \left(\frac{E}{2\beta} \right)^2} \right)^{1/3} \right)^2 \left(-\frac{d}{dE} \left(\frac{1}{1 + e^{\frac{E-E_F}{k_B T}}} \right) \right) dE. \quad (5)$$

This equation may be solved numerically by employing the partial integration method and using the simplification form, whereas $x = (E - \Delta)/k_B T$ and $\eta = (E_F - \Delta)/k_B T$, where η is normalized Fermi energy and $\Delta = qv_g/2$. Note that changing the gate voltage not only varies the band structure of TGN but also modifies the Fermi energy level (η). Hence, the general conductance model of TGN will be obtained as

$$\begin{aligned}
 G = N_2 G_2 = -N_2 \int_{-V}^{+V} & \left(\frac{2k_B T}{1 + e^{x-\eta}} \right) \times \left(\frac{-\frac{k_B T}{2\beta} - \frac{xk_B T + \Delta}{4\beta^2 \sqrt{-\frac{\alpha^3}{27\beta^3} + \frac{E^2}{4\beta^2}}}}{3 \left(-\frac{xk_B T + \Delta}{2\beta} - \sqrt{-\frac{\alpha^3}{27\beta^3} + \frac{(xk_B T + \Delta)^2}{4\beta^2}} \right)^{2/3}} \right. \\
 \times & \left. + \frac{-\frac{k_B T}{2\beta} + \frac{xk_B T + \Delta}{4\beta^2 \sqrt{-\frac{\alpha^3}{27\beta^3} + \frac{E^2}{4\beta^2}}}}{3 \left(-\frac{xk_B T + \Delta}{2\beta} + \sqrt{-\frac{\alpha^3}{27\beta^3} + \frac{(xk_B T + \Delta)^2}{4\beta^2}} \right)^{2/3}} \right) dx, \\
 & \times \left(\left(-\frac{xk_B T + \Delta}{2\beta} - \sqrt{-\frac{\alpha^3}{27\beta^3} + \frac{(xk_B T + \Delta)^2}{4\beta^2}} \right)^{1/3} \right. \\
 & \left. + \left(-\frac{xk_B T + \Delta}{2\beta} + \sqrt{-\frac{\alpha^3}{27\beta^3} + \frac{(xk_B T + \Delta)^2}{4\beta^2}} \right)^{1/3} \right)
 \end{aligned} \tag{6}$$

where V is the voltage between drain and source. Figure 4(a) shows conductance of TGN versus gate voltage (vg). It is clearly shown that the conductivity of TG increases by increasing the magnitude of gate voltage. However, temperature dependence of TGN conductance has been studied experimentally in Ref. 4. The measurement shows that minimum conductivity dramatically increases when temperature increases. This is comparable with BGN, in which similar thermal behavior is shown, while the minimum conductivity of monolayer graphene nanoribbon is nearly unchangeable with temperature changing.^{4,8} Similarly, based on the reported model, minimal conductivity increases as the temperature increases. Figure 4(a) shows the conductance of TGN in 100 K (blue line) and 300 K (red line), with which the temperature effect on conductivity of TGN is demonstrated. Note that the shift in the figure is for better illustration, meaning temperature does not shift the conductance. The Fermi energy distribution function is estimated to be one in degenerate limit meaning that the probability of the filling energy states is one.³⁵ Therefore, in degenerate condition, general conductance model can be

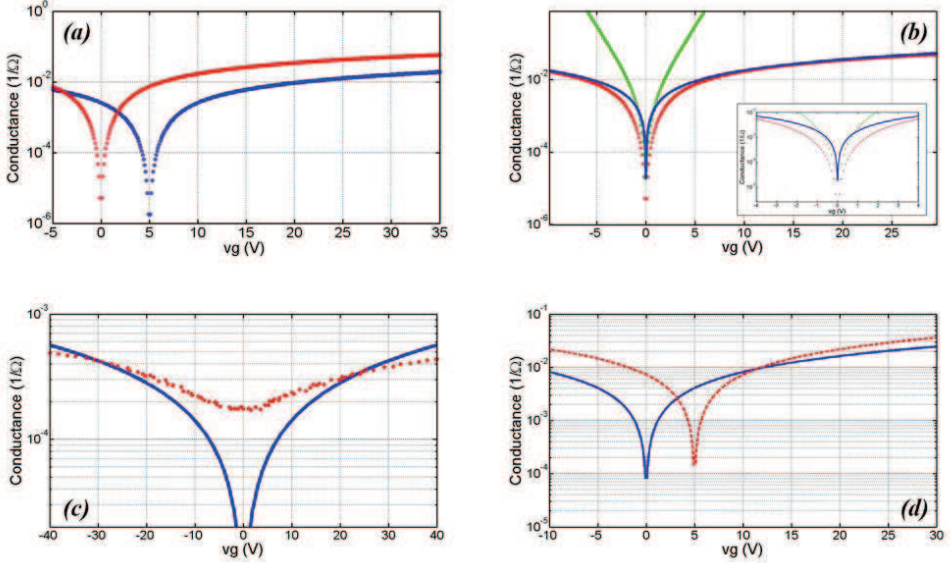


Fig. 4. (Color online) (a) Temperature dependence of TGN conductance. Red and blue line shows TGN conductance in 300 and 100 K (Numerical solution of general TGN conductance model based on Eq. (6)). (b) Analytical model of TGN conductance in degenerate condition (blue line) and Maxwell–Boltzmann approximation model of TGN conductance (green line) and general model of TGN conductance (red line). The inset shows the same figure but for small range of vg . (c) Conductance of TG versus gate voltage. Comparison of the presented model (blue line) and reported experimental data (red dots) indicates that better performance of ABA TGN-based transistor is predicted in degenerate regime. (d) Comparison between BGN conductance (red dashed line) and TGN conductance (blue solid line).

written as

$$G_D = -N_2 \int_{-V}^{+V} \left(\frac{-\frac{1}{\beta} - \frac{E}{2\beta^2 \sqrt{-\frac{\alpha^3}{27\beta^3} + \frac{E^2}{4\beta^2}}}}{3 \left(-\frac{E}{2\beta} - \sqrt{-\frac{\alpha^3}{27\beta^3} + \frac{E^2}{4\beta^2}} \right)^{2/3}} + \frac{-\frac{1}{\beta} + \frac{E}{2\beta^2 \sqrt{-\frac{\alpha^3}{27\beta^3} + \frac{E^2}{4\beta^2}}}}{3 \left(-\frac{E}{2\beta} + \sqrt{-\frac{\alpha^3}{27\beta^3} + \frac{E^2}{4\beta^2}} \right)^{2/3}} \right) \times \left(\left(-\frac{E}{2\beta} - \sqrt{-\frac{\alpha^3}{27\beta^3} + \frac{E^2}{4\beta^2}} \right)^{1/3} + \left(-\frac{E}{2\beta} + \sqrt{-\frac{\alpha^3}{27\beta^3} + \frac{E^2}{4\beta^2}} \right)^{1/3} \right) dE. \quad (7)$$

Fortunately, in the degenerate limit, the general model can be solved analytically [Eq. (8)], which illustrates accurate results in this regime. As shown in Fig. 4(b), the analytical solution of TGN conductance and the general solution of TGN conductance are in good agreement in degenerate limit (higher gate voltage) especially out of neutrality point where two curves are fitted.

$$G_D = N_2 \frac{\left(-\frac{9E}{\beta} - \sqrt{\frac{81E^2 - 12\alpha^3}{\beta^3}}\right)^{2/3} + \left(-\frac{9E}{\beta} + \sqrt{\frac{81E^2 - 12\alpha^3}{\beta^3}}\right)^{2/3}}{6.87}. \quad (8)$$

Yet, based on the good agreement between analytical model and general model, the analytical model can be employed as a conductance model to predict TGN behavior in TGN-based devices. In addition, it is expected that TGN operates in degenerate regime as a channel between drain and source. In contrary, applying the Maxwell–Boltzmann approximation to recalculate the conductance model of TGN, we find the conductance model in the non-degenerate condition. Figure 4(b) shows the conductance model of TGN in the non-degenerate regime (shown in green line) compared with the general model derived from Eq. (6), which can be utilized in neutrality point. As shown in Fig. 4(c), the experimental results of TG conductance (red dots)^{4,8} in $T = 50$ mK are in good agreements with theoretical calculations (blue dots) presented in this paper at the same temperature. We note that the presented model in the 1D form can be extracted into 2D form by employing width of TGN more than De-Broglie wavelength and this is also the reason why in the non-degenerate regime the presented model is far from the experimental data. The comparison between the presented model and the published data indicates that better performance of ABA TGN-based transistor is recommended in degenerate regime.

Considering the conductance model of BGN as a channel in BGNFET taken from Ref. 13, and TGN conductance model obtained in this paper, we demonstrated Fig. 4(d). It reveals that BGN conductivity (red dashed line) is more than TGN conductivity (blue solid line) in similar external applied electric field. However, presented conductance model can provide a better understanding toward the TGN field-effect transistor applications.

3. Conclusion

A single layer of carbon atoms in honeycomb lattice is known as Graphene. Multi-layer of graphene can be stacked differently depending on the horizontal shift of graphene. Common hexagonal structure in graphite is Bernal (ABA) stacking, in which the applied external electric field will change some amount of overlap of its conduction and valence bands resulting in a semimetal. In this paper, based on Landauer formula, we present the conductance model of ABA stack TGN (TG with width and thickness less than De-Broglie wavelength) as a field-effect transistor channel. TGN conductance can be estimated by either analytical model in

the degenerate regime out of neutrality point, or Maxwell–Boltzmann approximation in non-degenerate regime in neutrality point. The proposed model is in good agreement with the reported data from experiment, which illustrates that minimum conductivity dramatically increases as temperature increases. Our model also indicates that better performance of ABA TGN-based transistor can be seen in degenerate regime like what we expect in conventional semiconductors. Moreover, our model confirms that in similar condition, the conductivity of TGN is less than BGN as reported in some experiments.

Acknowledgment

The authors would like to acknowledge the financial support from Research University grant of the Ministry of Higher Education (MOHE), Malaysia. We also thank the Research Management Center (RMC) of Universiti Teknologi Malaysia (UTM) for providing excellent research environment to complete this work.

References

1. K. S. Novoselov *et al.*, *Science* **306** (2004) 666.
2. A. K. Geim and K. S. Novoselov, *Nat. Mater.* **6**(3) (2007) 183–191.
3. A. A. Avetisyan, B. Partoens and F. M. Peeters, *Phys. Rev. B* **81**(11) (2010) 115432.
4. M. F. Craciun *et al.*, *Nat. Nanotechnol.* **4**(6) (2009) 383–388.
5. J. H. Warner, *Nanotechnology* **21**(25) (2010) 255707.
6. J. A. Yan, W. Y. Ruan and M. Y. Chou, *Phys. Rev. B* **77**(12) (2008) 125401.
7. C. Berger *et al.*, *J. Phys. Chem. B* **108** (2004) 19912–19916.
8. W. J. Zhu *et al.*, *Phys. Rev. B* **80**(23) (2009) 235402.
9. P. Sutter *et al.*, *Nano Lett.* **9**(7) (2009) 2654–2660.
10. K. H. Ding, Z. G. Zhu and J. Berakdar, *J. Phys.: Condens. Matter* **21**(18) (2009).
11. M. Ezawa, *Physica E* **40**(2) (2007) 269–272.
12. M. T. Ahmadi *et al.*, *J. Nanomater.* **2010** (2010) 4.
13. H. Sadeghi *et al.*, *J. Comput. Theor. Nanosci.* **8**(10) (2011) 1993–1998.
14. M. Koshino and E. McCann, *Phys. Rev. B* **79**(12) (2009) 125443.
15. J. Guttinger *et al.*, *New J. Phys.* **10** (2008) 125029.
16. K. F. Mak, J. Shan and T. F. Heinz, *Phys. Rev Lett.* **104**(17) (2010) 176404.
17. F. Zhang *et al.*, *Phys. Rev. B* **82**(3) (2010) 035409.
18. C. L. Lu *et al.*, *Appl. Phys. Lett.* **89**(22) (2006).
19. E. McCann and M. Koshino, *Phys. Rev. B* **81**(24) (2010) 241409.
20. V. Ryzhii *et al.*, *J. Appl. Phys.* **103**(9) (2008) 094510–8.
21. P. N. Nirmalraj *et al.*, *Nano Lett.* **11**(1) (2011) 16–22.
22. W. Zhu, V. Perebeinos, M. Freitag and P. Avouris, *Phys. Rev. B* **80**(23) (2009) 235402.
23. G. M. Rutter *et al.*, *J. Vac. Sci. Technol. A* **26**(4) (2008) 938–943.
24. S. Russo *et al.*, *New J. Phys.* **11**(9) (2009) 095018.
25. A. A. Avetisyan, B. Partoens and F. M. Peeters, *Phys. Rev. B* **80**(19) (2009) 195401.
26. F. Guinea, A. H. C. Neto and N. M. R. Peres, *Phys. Rev. B* **73**(24) (2006) 245426.
27. S. Latil, V. Meunier and L. Henrard, *Phys. Rev. B* **76**(20) (2007) 201402(R).
28. B. Partoens and F. M. Peeters, *Phys. Rev. B* **74**(7) (2006) 075404.
29. T. Kat, *Perturbation Theory for Linear Operators*, Vol. 132 (Springer Verlag, 1995).

30. S. Datta, *Quantum Transport: Atom to Transistor* (Cambridge University Press, 2005).
31. S. Datta, *Electronic Transport in Mesoscopic Systems* (Cambridge University Press, 2002).
32. H. Y. Xu, T. Heinzel and I. V. Zozoulenko, *Phys. Rev. B* **80**(4) (2009) 045308.
33. M. Lundstrom and J. Guo, *Nanoscale Transistors: Device Physics, Modeling and Simulation* (Springer Verlag, 2006).
34. A. D. Polyainin, *Cubic Equation*, < <http://eqworld.ipmnet.ru/en/solutions/ae/ae0103.pdf> > (2004).
35. R. Pierret, *Advanced Semiconductor Fundamentals*, 2nd edn. (Prentice Hall, 2003).